

Quasiparticles at the verge of localization near the Mott metal-insulator transition in a two-dimensional material

J. Merino¹, M. Dumm², N. Drichko^{2,3}, M. Dressel², and Ross H. McKenzie⁴

¹ *Departamento de Física Teórica de la Materia Condensada, Universidad Autónoma de Madrid, Madrid 28049, Spain*

² *1. Physikalisches Institut, Universität Stuttgart, Pfaffenwaldring 57, 70550 Stuttgart, Germany*

³ *Ioffe Physico-Technical Institute, Russian Academy of Science, 194021 St.Petersburg, Russia*

⁴ *Physics Department, University of Queensland, Brisbane 4072, Australia*

(Dated: August 31, 2018)

The dynamics of charge carriers close to the Mott transition is explored theoretically and experimentally in the quasi two-dimensional organic charge-transfer salt, κ -(BEDT-TTF)₂Cu[N(CN)₂]-Br_xCl_{1-x}, with varying Br content. The frequency dependence of the conductivity deviates significantly from simple Drude model behavior: there is a strong redistribution of spectral weight as the Mott transition is approached and with temperature. The effective mass of the quasiparticles increases considerably when coming close to the insulating phase. A dynamical mean-field-theory treatment of the relevant Hubbard model gives a good quantitative description of the experimental data.

Understanding strongly correlated electron materials such as the high- T_c cuprate superconductors, heavy fermions, transition metal oxides, and organic superconductors is a significant theoretical challenge. Optical conductivity measurements are a powerful probe of the competition between the itineracy and localization of charge carriers [1, 2, 3, 4]. Unlike in elemental metals, a large redistribution of spectral weight (SW) occurs with variation in the Coulomb interaction and/or temperature [3, 4, 5, 6, 7]. The simple Drude model [1] fails to describe spectra in these systems, despite its success in conventional metals. In this Letter, we present a combined theoretical and experimental analysis of the redistribution of SW that occurs as the Mott metal-insulator transition is approached in a two-dimensional material.

The κ -family of layered organic superconductors based on the bis-(ethylenedithio)tetrathiafulvalene (BEDT-TTF) molecules [8] have conduction bands which are effectively half filled (due to dimerization of neighboring BEDT-TTF molecules). As the on-site Coulomb repulsion U is comparable to the bandwidth W , these materials are ideal systems to explore the bandwidth controlled Mott metal-insulator transition (MIT) in two dimensions. Measurements of the DC conductivity have been made as the materials tuned through the MIT via chemical substitution, pressure, magnetic field, and/or temperature [9, 10]. Much less is known about the charge-carriers dynamics in these systems close to the MIT [6, 11, 12, 13]. The optical conductivity calculated from a dynamical mean-field theory (DMFT) [14] treatment of the relevant Hubbard model is compared with optical spectra of single crystals of κ -(BEDT-TTF)₂Cu[N(CN)₂]-Br_xCl_{1-x}. Partial substitution of Br by Cl in the anion layer increases the effective Coulomb repulsion U/W , and drives the system across the metal-insulator phase boundary, which is at $x \simeq 0.7$ [15].

The simplest strongly correlated electron model for the conducting layers of the κ -(BEDT-TTF)₂X family is a Hubbard model on a frustrated square lattice at half filling [17]:

$$H = -t_2 \sum_{\langle ij \rangle, \sigma} (c_{i\sigma}^\dagger c_{j\sigma} + c_{j\sigma}^\dagger c_{i\sigma}) - t_1 \sum_{\langle\langle ij \rangle\rangle, \sigma} (c_{i\sigma}^\dagger c_{j\sigma} + c_{j\sigma}^\dagger c_{i\sigma}) + U \sum_i n_{i\uparrow} n_{i\downarrow} - \mu \sum_{i\sigma} c_{i\sigma}^\dagger c_{i\sigma} \quad , \quad (1)$$

where σ is the spin index, t_1 describes hopping along one diagonal of the square plaquettes, t_2 describes hopping around the plaquettes, and $c_{i\sigma}^\dagger$ and $c_{i\sigma}$ are hole creation and destruction operators on the antibonding orbitals of BEDT-TTF dimers. The non-interacting model ($U = 0$) has a dispersion relation:

$$\epsilon(\mathbf{k}) = -2t_2[\cos(k_x d) + \cos(k_y d)] - 2t_1 \cos((k_x + k_y)d) \quad (2)$$

with d the nearest-neighbor dimer distance. We take the nearest-neighbor hopping amplitudes to be $t_2 = -0.03$ eV and $t_1 = 0.8t_2$ which leads to a non-interacting bandwidth of $W \approx 0.3$ eV, comparable to values from density functional theory (DFT) calculations [18].

Previous studies of model (1) based on DMFT calculations [19] and its cluster extensions [20] considered the Mott-Hubbard metal-insulator transition driven by U/W . Anomalous transport properties observed in κ -(BEDT-TTF)₂X [9], such as the non-monotonic temperature dependence of the DC resistivity, thermopower, and Hall coefficient agrees with DMFT, which predicts the gradual destruction of quasiparticles with increasing temperature, T . This leads to a crossover from Fermi-liquid behavior at low T to ‘bad’ metallic behavior for $T > T^*$, with $T^* \ll W$ [19]. Signatures of the gradual destruction of quasiparticles as the temperature is increased above $T^* \approx 100$ K can be seen in Fig. 1, which shows the frequency dependence of the real part

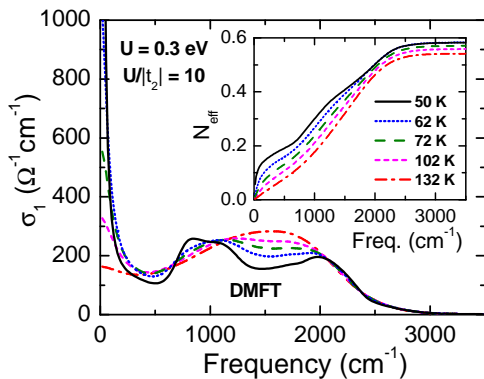


FIG. 1: (Color online). Frequency dependence of the optical conductivity at several temperatures. Calculations are based on a DMFT treatment of the Hubbard model on the anisotropic triangular lattice. For $U = 0.3$ eV, a gradual suppression of the Drude peak occurs with increasing temperature. Above the coherence temperature, $T^* \approx 100$ K, the Drude peak disappears, due to the destruction of Fermi liquid quasiparticles. The inset shows the effective number of charge carriers $N_{\text{eff}}(\omega)$ per lattice site, calculated from the spectrum using Eqns. (4) and (5).

of the optical conductivity $\sigma_1(\omega)$ for several temperatures. The results are obtained from DMFT using iterative perturbation theory [14]. At the lowest temperature three features are found: a Drude peak at $\omega = 0$, a broad absorption band at $\omega \approx 2000 \text{ cm}^{-1} \sim U$, and a band at $U/2$. The broad band is a result of electronic transitions between the Hubbard bands separated by $U = 10|t_2| = 0.3$ eV, while the band at $U/2$ results from transitions between the quasiparticle peak and Hubbard bands.

Single crystals of $\kappa\text{-(BEDT-TTF)}_2\text{Cu}[\text{N}(\text{CN})_2]\text{-Br}_x\text{Cl}_{1-x}$ are investigated by polarized reflectivity spectroscopy in a broad frequency and temperature range (for details see Ref. 15). The optical response can be separated into contributions from correlated charge carriers, intradimer charge-transfer transitions, and vibronic modes activated by these charge-transfer transitions. While the spectra of all the compounds are similar at high temperatures, a clear distinction can be made below 50 K. A Drude peak is present for a Br content of $x = 0.73, 0.85$, and 0.9 indicating metallic behavior. In contrast, no Drude peak is seen in the materials with $x = 0$ and 0.4 , consistent with a Mott insulating ground state [15]. In order to compare the measurements to DMFT calculations, we followed the procedure used in Ref. 15 to subtract the contributions of intradimer electronic transitions (around 3400 cm^{-1}) and vibrational features from the optical conductivity spectra, since the associated physics is not incorporated in the model (1).

The optical conductivity, $\sigma_1(\omega)$, is shown in Fig. 2 for the compound with 73% Br. We confine ourselves to

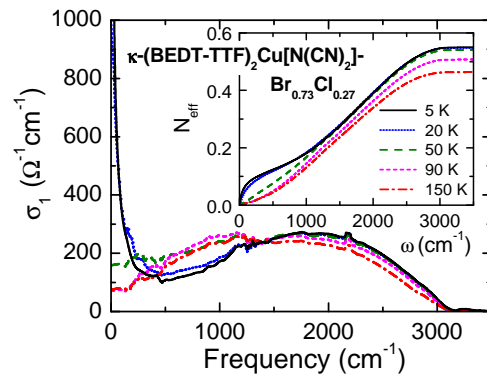


FIG. 2: (Color online). Frequency dependence of the optical conductivity due to the correlated charge carriers of $\kappa\text{-(BEDT-TTF)}_2\text{Cu}[\text{N}(\text{CN})_2]\text{Br}_{0.73}\text{Cl}_{0.27}$. Experimental data [15] are shown for conductivity in the layers ($E \parallel c$) at different temperatures. This data compares favourably with theoretical calculations presented in Fig. 1. The inset shows the effective number of charge carriers $N_{\text{eff}}(\omega)$ per dimer.

the polarization $E \parallel c$; [the crystal c -axis is parallel to the diagonal $k_y = k_x$ in the model (2)] similar results are obtained along the second intralayer crystal axis. At $T = 150$ K, one broad absorption feature is observed centered around 2000 cm^{-1} . When the sample is cooled down, the SW shifts towards lower frequencies and below 50 K a narrow Drude-like component develops. Interestingly, the overall SW decreases for $T > 50$ K. The redistribution of spectral weight with varying temperature, observed in Fig. 2 is consistent with the calculations shown in Fig. 1. The agreement is particularly impressive as there are really only two parameters in the calculation, the magnitude of t_2 (which sets the vertical scale) and the ratio U/t_2 which determines the relative weight in the Drude peak. However, we do note two discrepancies. First, the band at $\omega \sim U/2$ does not appear in the experimental data. Second, the temperature scale on which the Drude weight collapses is about a factor of two larger in the calculation than in the experiment. Such discrepancies are not unusual in systems exhibiting Kondo physics, as occurs in DMFT [14].

To describe the redistribution of spectral weight with varying temperature and correlation strength, it is useful to consider restricted f-sum rule [2, 21] based on the integral:

$$I_\sigma(\Lambda) \equiv \int_0^\Lambda \sigma_1(\omega) d\omega \equiv \frac{\pi n e^2}{2m_{\text{sum}}^*} \quad (3)$$

where Λ is a high-frequency cut-off which excludes interband transitions (we take $\Lambda = 3500 \text{ cm}^{-1}$), e is the electronic charge, n is the total electron density (excluding filled bands) and the last identity defines a particular effective mass m_{sum}^* . Expression (3) can be compared to the full f-sum rule which is independent of temperature

and the strength of the correlations [1, 2]. When the conductivity is integrated up to infinity, it can be related to the plasma frequency of an electron gas with the total electron density.

In order to make more detailed statements we have to consider the effective mass and effective carrier concentration separately. For a single two-dimensional metallic band of *non-interacting* electrons all the spectral weight is in the Drude peak and the sum rule is

$$I_\sigma(\Lambda) = \frac{\pi e^2}{b} \int_{occ} \frac{d^2\mathbf{k}}{(2\pi\hbar)^2} \frac{\partial^2 \epsilon(\mathbf{k})}{\partial k_c^2} \equiv \frac{\pi n e^2}{2m_{b,opt}} \quad , \quad (4)$$

where b is the interlayer spacing, and integral 3 is over all the occupied states (i.e. the Fermi sea). The last equality defines an optical band mass, $m_{b,opt}$ [22]. For the tight-binding model (2) at half-filling, evaluating Eq. (4), with $t_2 = -0.03$ eV and $t_1 = 0.8t_2$ yields an optical band mass, $m_{b,opt} = 2.3m_e$. This agrees very well with $m_{b,opt} = 2.5m_e$ obtained from our experimental data [15, 16].

For a Hubbard model with *only nearest-neighbor* hopping on an isotropic lattice this integral is proportional to the expectation value of the kinetic-energy operator [2, 5, 21]. This sum rule even holds in the absence of a Drude response and in the Mott insulating phase. The total spectral weight – as calculated in Eq. (3) – can then vary with temperature and the strength of the electronic correlations [5]. However, we should point out that although this connection with the kinetic energy will hold qualitatively for our Hubbard model, it will not hold quantitatively because the system of interest is spatially anisotropic. In the Hubbard model (1) there are next-nearest neighbor terms (t_1) which are comparable to the nearest neighbor terms and frustrate the kinetic energy.

For the further analysis of the effects of electronic correlations on the charge-carrier kinetic energy, we rewrite Eq. (3) and define a frequency-dependent carrier density:

$$N_{\text{eff}}(\omega) = \frac{2m_{b,opt}}{\pi e^2} \int_0^\omega \sigma_1(\omega') d\omega' \quad . \quad (5)$$

where at infinite frequencies N_{eff} is equal to the number of charge carriers on a dimer (f-sum rule), while deviation from this value indicate the change in kinetic energy; i.e. the influence of electronic correlations. For a weakly correlated metal, $N_{\text{eff}}(\omega)$ increases rapidly from zero to unity once ω becomes larger than the intraband scattering rate, because almost all the spectral weight is in the Drude peak (see the $U = 0.06$ eV curve in Fig. 3). As U/W is increased, both in theory and experiment (Figs. 3 and 4), SW is transferred to higher frequencies and $N_{\text{eff}}(\omega)$ saturates above frequencies of about $\omega \sim U$. The absolute value of N_{eff} is substantially suppressed. Qualitatively, the reduction in the total spectral weight with increasing correlations is due to the diminishing kinetic energy of the charge carriers.

In the inset of Fig. 1, $N_{\text{eff}}(\omega)$ evaluated using DMFT with $U = 0.3$ eV is plotted for different temperatures.

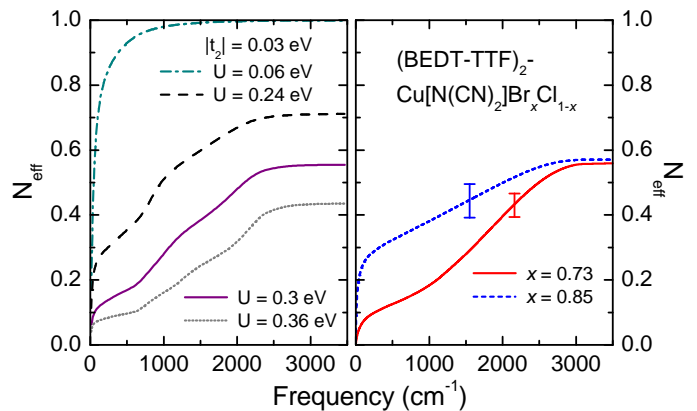


FIG. 3: (Color online). Effective charge-carrier number per (BEDT-TTF)₂ dimer approaching the Mott transition. In the left panel the results of a DMFT calculation of $N_{\text{eff}}(\omega)$ (at a temperature of 50K) show how the spectral weight is redistributed as one approaches the transition to the Mott insulating phase which occurs at $U = 15|t_2| = 0.45$ eV. The SW redistribution and saturation of $N_{\text{eff}}(\omega)$ is in agreement with the experimental data for κ -(BEDT-TTF)₂Cu[N(CN)₂]Br_xCl_{1-x} for $x = 0.73, 0.85$ (at low temperature) shown in the right panel. Typical error bars for the experimental data are shown.

At large frequencies, the integrated spectrum saturates to about 0.6. The calculations are consistent with experimental results for κ -(BEDT-TTF)₂Cu[N(CN)₂]Br_{0.73}Cl_{0.27}, shown in the inset of Fig. 2 and the right panel of Fig. 3. With increasing temperature, $N_{\text{eff}}(\omega)$ is suppressed at low frequencies and spectral weight is transferred to high ω , whereas the total spectral weight of the correlated carriers is not conserved because of the gradual destruction of quasiparticles with increasing temperature.

For a more sophisticated analysis of the mass enhancement of the correlated carriers, the frequency dependent mass renormalization can be quantified with the generalized Drude model [1, 23]:

$$\sigma(\omega) = \sigma_1(\omega) + i\sigma_2(\omega) = \frac{(2/\pi)I_\sigma(\Lambda)}{1/\tau(\omega) - i\omega m^*(\omega)/m_{b,opt}} \quad , \quad (6)$$

where $m^*(\omega)$ and $1/\tau(\omega)$ are a frequency dependent optical effective mass and scattering rate, respectively. At high frequencies the effective mass becomes equal to the optical band mass, since at high frequencies, $\sigma(\omega)$ is dominated by the imaginary part. The frequency dependences of this scattering-rate and effective-mass enhancement are plotted in Fig. 4. A sharp drop in $m^*(\omega)$ and a peak in $1/\tau(\omega)$ both occur in DMFT at a frequency, ω_c as shown in Figs. 4(a) and 4(b). Below a frequency scale, ω^* Fermi liquid behavior, i.e., $1/\tau(\omega) \propto \omega^2$, occurs. For $U = 0.3$ eV, the DMFT calculations give: $\omega^* \approx 400$ cm⁻¹ (inset of Fig. 4a) in good agreement with the experimental value. Both ω_c and ω^* are shifted to lower frequencies

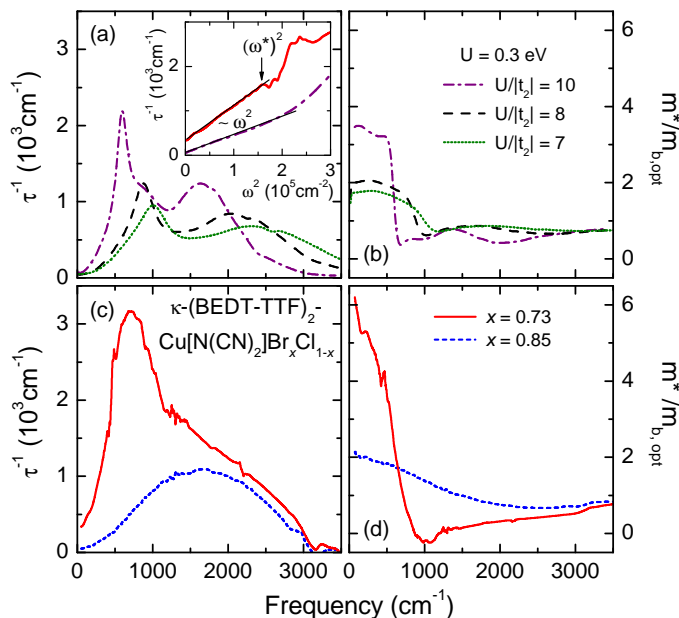


FIG. 4: (Color online). Frequency dependence of the scattering rate and effective mass extracted from an extended Drude model analysis of the optical conductivity. (a) and (b) shows the results of DMFT calculations for different U/W and $T = 50\text{K}$. (c) and (d) show the experimental results for the same quantities at $T = 5\text{K}$. The inset of (a) shows how below a frequency $\omega^* \approx 400\text{ cm}^{-1}$ the scattering rate found for both experiment and theory has the quadratic frequency dependence expected for Fermi liquid quasiparticles. Clearly as the Mott insulating phase is approached the effective mass and the scattering rate increase significantly.

with increasing U/W , consistent with the shift observed as x decreases from 0.85 to 0.73. The collapse of the effective mass enhancement at high frequencies is reminiscent of what occurs in heavy fermion compounds[4] and the ‘kink’ seen in ARPES experiments on cuprate superconductors and has recently been argued to be a ubiquitous feature of strongly correlated electron systems [24, 25].

The large increase in the effective optical mass as the system comes closer to the Mott insulating phase (due to increasing Cl content) is consistent with the large mass renormalization expected from Brinkman-Rice and DMFT pictures[14]. This is distinctly different from what occurs in doped Mott insulators, such as the cuprates, for which the effective mass deduced from an extended Drude model analysis is weakly dependent on the doping as the Mott insulating phase is approached [26, 27]. For $U/t_2 = 2, 8, 10, 12$, the enhancements in the effective mass of the Fermi liquid quasiparticles calculated from DMFT are $m^*/m_{b,\text{opt}} = 1.1, 2.1, 3.1, \text{ and } 4.1$, respectively.

In conclusion, quasiparticles at the verge of localization in $\kappa\text{-(BEDT-TTF)}_2\text{Cu}[\text{N}(\text{CN})_2]\text{Br}_x\text{Cl}_{1-x}$ display a sizeable redistribution of spectral weight as the temper-

ature and x vary. The strong local Coulomb correlations developing close to the Mott transition at $x = 0.7$ lead to spectral-weight transfer from low to high frequencies. The effective masses extracted from optical data are strongly enhanced approaching the Mott transition, in contrast to doped Mott insulators. These effects lead to the destruction of coherent excitations above a frequency scale, ω^* .

We thank P. Batail, C. Meziere, D. Faltermeier, and B.J. Powell for their contributions to this work. The project was supported by the Ramón y Cajal program from MCyT in Spain, the MEC under contract CTQ2005-09385-C03-03, the grant ‘Leading Scientific Schools’ NSH-5596.2006.2, the Deutsche Forschungsgemeinschaft, and the Australian Research Council.

-
- [1] M. Dressel and G. Grüner, *Electrodynamics of Solids* (Cambridge University Press, Cambridge, 2002).
 - [2] D. van der Marel, in: *Strong interactions in low dimensions*, edited by D. Baeriswyl and L. Degiorgi, (Kluwer, Dordrecht, 2004).
 - [3] D.N. Basov and T. Timusk, *Rev. Mod. Phys.* **77**, 721 (2005).
 - [4] L. Degiorgi, *Rev. Mod. Phys.* **71**, 687 (1999).
 - [5] M.J. Rozenberg *et al.*, *Phys. Rev. Lett.* **75**, 105 (1995).
 - [6] C. S. Jacobsen, *et al.*, *Phys. Rev. B* **35** 9605 (1987); C. S. Jacobsen, *J. Phys. C: Sol. Stat. Phys.* **19** 5643 (1986).
 - [7] V. Vescoli *et al.*, *Eur. Phys. J. B* **3**, 149 (1998).
 - [8] T. Ishiguro, K. Yamaji, and G. Saito, *Organic Superconductors*, 2nd edition (Springer, Berlin, 2001).
 - [9] P. Limelette *et al.*, *Phys. Rev. Lett.* **91**, 016401 (2003).
 - [10] F. Kagawa *et al.*, *Nature* **436**, 534 (2005).
 - [11] J. E. Eldridge *et al.*, *Solid State Commun.* **79**, 583 (1991); K. Kornelsen *et al.*, *ibid.* **81**, 343 (1992).
 - [12] T. Sasaki *et al.* *Phys. Rev. B* **69**, 064508 (2004).
 - [13] M. Nam *et al.*, *Nature* **449**, 584 (2007).
 - [14] A. Georges *et al.*, *Rev. Mod. Phys.* **68**, 13 (1996).
 - [15] D. Faltermeier *et al.*, *Phys. Rev. B* **76**, 165113 (2007).
 - [16] M. Dumm, *et. al.* to be published.
 - [17] B.J. Powell and R.H. McKenzie, *J. Phys.: Cond. Matter.* **18**, R827 (2006).
 - [18] J. Merino and R.H. McKenzie, *Phys. Rev. B* **62**, 2416 (2000).
 - [19] J. Merino and R. H. McKenzie, *Phys. Rev. B* **61**, 7996 (2000).
 - [20] O. Parcollet *et al.*, *Phys. Rev. Lett.* **92**, 226402 (2004).
 - [21] P. F. Maldague, *Phys. Rev. B* **16**, 2437 (1977).
 - [22] We want to stress that for a non-parabolic band the optical band mass $m_{b,\text{opt}}$ is *not necessarily* equal to the band mass associated with the cyclotron mass and the linear coefficient of the temperature dependence of the electronic heat capacity; both of the latter being proportional to the density of states at the Fermi energy [18]
 - [23] A.V. Puchkov *et al.*, *J. Phys.: Condens. Matter* **8**, 10049 (1996).
 - [24] K. Byczuk *et al.*, *Nature Physics* **3**, 168 (2007).
 - [25] M.M. Zemljic *et al.*, cond-mat/0706.1156; A. Macridin *et al.*, cond-mat/0706.01429.

- [26] S. Uchida *et al.*, Phys. Rev. B **43**, 7942 (1991); W.J. Padilla *et al.*, Phys. Rev. B **72**, 060511 (2005). (2007); F. Carbone *et al.*, Phys. Rev. B **74**, 064510 (2006).
- [27] K. Haule and G. Kotliar, Europhys. Lett. **77**, 27007